# Numerical Benchmark for the Deep-Burn Modular Helium-Cooled Reactor (DB-MHR)

T. A. Taiwo and T. K. Kim
*Argonne National Laboratory, 9700 South Cass Avenue Argonne, IL 60439, U.S.A.*
L. Buiron and F. Varaine
*DEN/DER/SPRC/LEDC, CEA Cadarache, St. Paul lez Durance, France*

## Abstract

Numerical benchmark problems for the deep-burn concept based on the prismatic modular helium-cooled reactor design (a Very High Temperature Reactor (VHTR)) are specified for joint analysis by U.S. national laboratories and industry and the French CEA. The results obtained with deterministic and Monte Carlo codes have been inter-compared and used to confirm the underlying feature of the DB-MHR concept (high transuranics consumption). The results are also used to evaluate the impact of differences in code methodologies and nuclear data files on the code predictions for DB-MHR core physics parameters. The code packages of the participating organizations (ANL and CEA) are found to give very similar results.

***KEYWORDS: Deep-burn, transuranics, benchmark.***

## 1. Introduction

For the purpose of burning plutonium (Pu), neptunium (Np), and americium (Am) nuclides, the Deep-Burn, Modular Helium-cooled Reactor (DB-MHR) concept has been proposed by General Atomics (GA), based on the technologies of the graphite moderated Gas-Turbine, Modular Helium-cooled Reactor (GT-MHR). [1,2] The essential feature of this transmutation concept is the use of coated fuel particles that are considered strong and highly resistant to irradiation, and potentially a durable waste form. The transuranics (TRU) material formed into fuel particles could be irradiated for a long time in the DB-MHR in order to obtain a very high TRU consumption (in particular fissile nuclides).

Since the DB-MHR core design has not been deployed and used internationally, it is imperative that the design and licensing evaluations to support the concept be done with codes that have been validated and verified. To provide some confidence in the preliminary evaluations of the DB-MHR cores, numerical benchmark problems for the deep-burn concept have been specified for joint analysis by U.S. national laboratories and industry and the French CEA.

This numerical benchmark has been organized into three phases and simplifying assumptions have made the benchmark problems tractable for meaningful comparison of results. The descriptions of the problem source and benchmark phases are presented in Section 2. The methodologies used by the Argonne and CEA participants in the benchmark are summarized in Section 3. Section 4 contains the results obtained by the participants for the different phases. Conclusions are given in Section 5.

# 2. Problem Source and Benchmark Definition

## 2.1 Description of DB-MHR Fuel Element

The DB-MHR standard fuel element design is based on that for the General Atomics (GA) gas-turbine modular helium-cooled reactor. [2] The fuel element is a hexagonal prismatic block of graphite containing channels (holes) for the fuel and burnable poison compacts and coolant passage. The fuel element flat-to-flat width is 35.9969 cm (the gap between the fuel elements is ignored in this study to simplify the problem). The principal fuel element structural material is graphite.

Figure 1 contains a schematic of a standard fuel element containing only fuel compacts and coolant channels. Burnable poison will most certainly be used for compensation of the burnup reactivity and control of the power peaking, but has not been specified in this model; this power-peak control feature is particularly important if an annular core design is used for passive decay heat removal and core safety reasons.

**Figure 1:** Standard Fuel Element (Left) and Radial View of Whole-Core (Right).

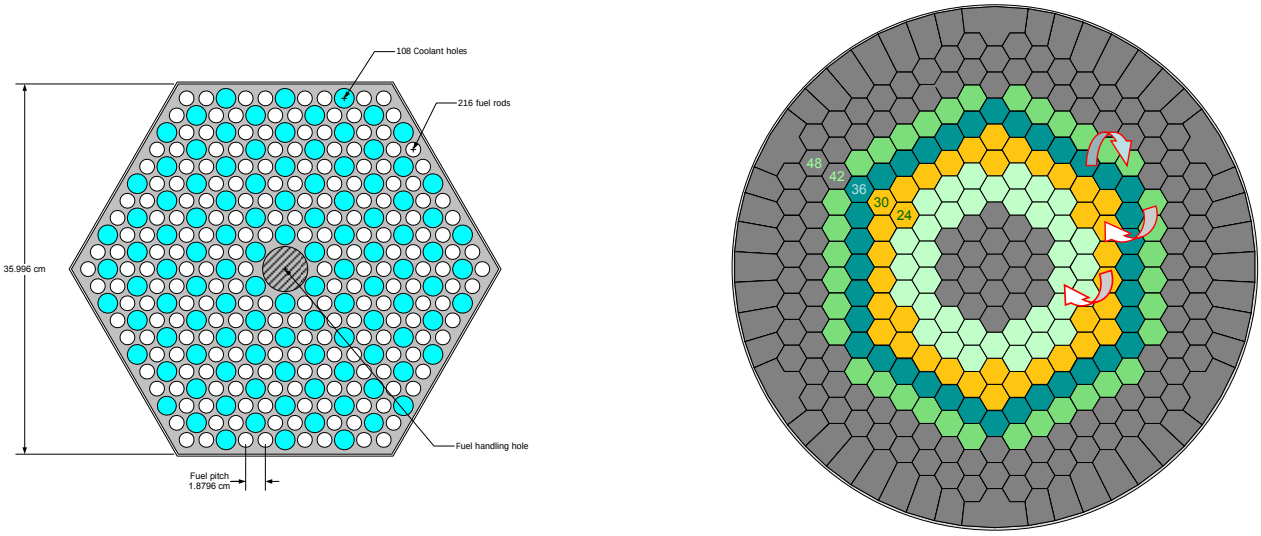


It is assumed that the fuel compacts in the fuel element are of the same kind. The fuel compact is a graphite medium, called matrix, in which coated fuel particles (CFPs) are dispersed. This fuel compact has significant resonance shielding effect that must be represented in the physics model. The impact of not representing this important effect will be evaluated in this study. The fuel particle, called TRISO fuel, contains multiple layers: fuel particle in the center, buffer zone layer, inner pyrolytic carbon layer, SiC layer, and the outer pyrolytic carbon layer.

Each compact has a diameter of 1.245 cm and a height of 4.93 cm. The fuel element has 216 fuel compact holes including those used for six lumped burnable poison rods (occupied by fuel compacts in current problem) and 108 coolant holes. The pitch of the coolant hole or fuel compact is 1.8796 cm and the radii of the fuel compact and fuel holes are 0.6223 and 0.6350 cm, respectively. The 108 coolant holes have a diameter of 1.5875 cm. A fuel handling hole (depth of 19% length of element) exists at the center of the fuel element. To simplify the problem, the

central fuel handling hole is modeled using 7 small hexagons having 81% density of the graphite block. The flat-to-flat width of these small hexagons is 1.8796 cm. Various fuel kernel diameters have been proposed by GA to improve the TRU consumption, but the kernel diameter is fixed as 200 μm in this study.

Table 1 is a summary of the geometry dimensions for the DB-MHR fuel element and core, and also contains information on the materials.

**Table 1:** Design Data for the DB-MHR Core.

| | Design parameter | Unit | Value |
|---|---|---|---|
| Core | Thermal Power | MWt | 600 |
| | Power density | $W/cm^3$ | 4.7 |
| | Specific power density | W/g | 501.3 |
| | Number of columns | - | 144 |
| | Number of blocks per column | - | 10 |
| | Fuel form | - | $(TRU)O_{1.7}$ |
| | Number of batch | - | 4 |
| | Number of columns per batch | - | 36 |
| | Coolant inlet/outlet temperature | $^oC$ | 490/850 |
| | Boron impurity in graphite | ppm | 1.5 |
| Fuel Column | Width of column | cm | 35.9969 |
| | Number of fuel pins | - | 216 |
| | Number of coolant holes | - | 108 |
| | Height | cm | 79.3 |
| Fuel Cell | Pitch of fuel cell | cm | 1.8796 |
| | Radius of fuel hole | cm | 0.635 |
| | Radius of fuel compact | cm | 0.6225 |
| | Radius of coolant hole | cm | 0.79375 |
| | Packing fraction | % | 20 |
| Particle Size | Kernel diameter | μm | 200 |
| | Buffer thickness | μm | 150 |
| | IPC thickness | μm | 35 |
| | SiC thickness | μm | 35 |
| | OPC thickness | μm | 40 |
| Density | Kernel | $g/cm^3$ | 10.36 |
| | Buffer | | 1.00 |
| | IPC | | 1.87 |
| | SiC | | 3.20 |
| | OPC | | 1.87 |
| | Fuel compact | | 1.74 |
| | Graphite block | | 1.74 |
| Heavy Metal Vector | Np-237 | % | 4.5941 |
| | Pu-238 | | 1.3340 |
| | Pu-239 | | 50.9975 |
| | Pu-240 | | 20.7970 |
| | Pu-241 | | 7.5689 |
| | Pu-242 | | 4.9457 |
| | Am-241 | | 8.2207 |
| | Am-242m | | 0.0304 |
| | Am-243 | | 1.5118 |

## 2.2 Description of DB-MHR Core

The core design for the deep-burnup concept has been developed using the primary design features of the General Atomics GT-MHR with modifications to improve fuel transmutation in a thermal reactor design (mainly different fuel type and CFP dimensions). The core considered for this benchmark is comprised of standard fuel elements and reflector block. Figure 1 contains the radial layout of the DB-MHR core.

The annular active core zone contains fuel columns. Each column is made up of 10 fuel elements stacked end-to-end in the axial direction. The active core zone is surrounded radially by an inner reflector zone and an outer reflector zone. Top and bottom reflectors also surround this active core zone in the axial direction. Since each fuel element has a height of 79.3 cm, the active core height is 793 cm.

The whole-core schematic in Fig. 1 has been developed for the specification of the depletion study. The gray hexagons denote the inner and outer graphite reflectors and other colored hexagons denote the active core regions. There are four colored "rings" because a four-batch fuel management scheme has been considered. These rings are for the four fuel batches (ages) contained in the equilibrium cycle. Each ring contains 36 fuel columns (for a total of 144 fuel columns or 1440 fuel elements in the core). In the fuel management scheme, fuel is loaded into one of the rings and then shuffled to the other rings at the beginning of subsequent cycles (BOCs).

## 2.3 Benchmark Phases

This numerical benchmark has been organized into three phases. Simplifying assumptions have made the benchmark problem tractable for meaningful comparison of results. For example, only the standard assembly type (containing fuel compacts) and reflector element have been defined. Additionally, the one-pass concept only will be considered to verify the ~60% consumption level that has been indicated by the DB-MHR design team; note that GA has also defined two- and multi-pass (recycle) concepts using transuranics from pressurized light water reactor spent nuclear fuel cooled for a short period (5 to 30 years). Based on the simplifying assumptions, the data contained in Table 1 have been used to derive number densities for the core compositions. These are summarized in Table 2. The specifications for the benchmark phases are discussed in the following subsections.

### *2.3.1 Phase 1: Problem for DB-MHR Fuel Element (Assembly) at Cold Condition*

This problem is based on a DB-MHR fuel element design at the cold condition (i.e., temperature of all materials is specified as 21$^{o}$C). The problem allows the deterministic code results to be compared with Monte Carlo code results. To obtain accurate results for this phase (and Phase 2), the fuel compact (fuel particle and matrix) heterogeneity must be modeled along with the other heterogeneity effects. The packing fraction (ratio of CFP volume to total compact volume) is specified as 20%. Impurity levels of B-10 in the graphite have also been utilized.

### *2.3.2 Phase 2: Depletion Problem for Fuel Element at Hot Condition*

The problem definition allows the intercomparison of nuclide densities and temperature reactivity defect predicted by lattice depletion codes used for generating cross sections for the whole-core analysis code system. This is a lattice depletion problem based on the DB-MHR element design at the hot condition. The same compositions and geometry information specified

for Phase 1 is employed for the initial state. The hot condition temperatures corresponding to this state are: fuel, buffer, inner and outer PyC and SiC at 1000°C and the graphite block at 800°C. A constant specific power density of 501.3 W/g is specified for the irradiation period. This specific power density corresponds to a power level of 600 MWt for the DB-MHR core.

**Table 2:** Material Composition Data for Lattice Calculation.

| Nuclide | Fuel | Buffer | Inner/Outer PyC | SiC | Graphite Block | Fuel Handling hole | Inner/Outer Reflector | Top/Bottom Reflector |
|---|---|---|---|---|---|---|---|---|
| Am241 | 1.91110E-03 | | | | | | | |
| Am242m | 7.03744E-06 | | | | | | | |
| Am243 | 3.48550E-04 | | | | | | | |
| Np237 | 1.08607E-03 | | | | | | | |
| Pu238 | 3.14026E-04 | | | | | | | |
| Pu239 | 1.19549E-02 | | | | | | | |
| Pu240 | 4.85493E-03 | | | | | | | |
| Pu241 | 1.75957E-03 | | | | | | | |
| Pu242 | 1.14497E-03 | | | | | | | |
| O | 3.97716E-02 | | | | | | | |
| B10 | | 1.6627E-08 | 3.1093E-08 | 1.5928E-08 | 2.8932E-08 | 2.3435E-08 | - | - |
| C | | 5.0184E-02 | 9.3844E-02 | 4.8074E-02 | 8.7334E-02 | 8.0741E-02 | 8.7334E-02 | 7.1030E-02 |
| Si | | | | 4.8074E-02 | | | | |

*2.3.3 Phase 3: Whole-core Depletion Problem*

This is a whole-core depletion problem based on a simplified R-Z geometry depletion model for the DB-MHR and is to be used to determine primary core characteristics (e.g., criticality and TRU consumption level for the equilibrium state). The cross sections derived from the hot-condition fuel element design in Phase 2, should be used for the problem. For this phase, it is assumed that the graphite-block cross sections from the fuel element calculation are adequate for use for the reflector zones. This is only an approximation for the DB-MHR core design, but is sufficient for the purpose of this benchmark exercise. Note that an extended calculation is required for the generation of both core and reflector cross sections. Future benchmarks could include a phase for the generation of cross sections using extended calculations.

The core dimensions, including for the four fuel rings (4 fuel batches) and the axial and radial reflectors, are shown in Fig. 2. Numbering the rings from 1 to 4, starting from the inner ring, the fuel is first loaded into Ring 3, and then shuffled sequentially at the beginning of subsequent cycles into Ring 4, Ring 2, and Ring 1. No axial shuffling is done in this case. The equilibrium core data is requested. The cycle length is specified as 286 days.

*2.3.4 Expected Benchmark Results*

The expected results for the fuel element at cold condition include the multiplication factor, magnitude of the double heterogeneity effect, neutron spectrum, and power distribution. At the elevated temperature condition, values of the fuel element multiplication factor, nuclide densities, power distribution, spectrum and temperature reactivity defect, as function of burnup are requested. The core multiplication factor at the beginning and end of the equilibrium cycle, charge and discharge nuclide masses, and TRU consumption level are additionally requested.

**Figure 2:** DB-MHR R-Z Model; Radial (Left) and Axial Views.

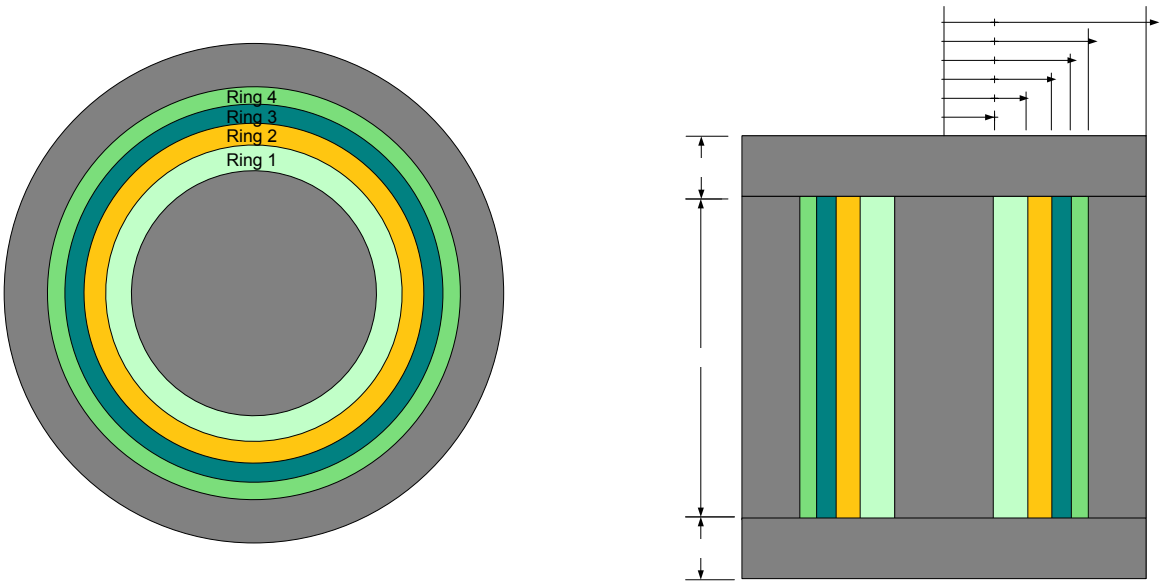


## 3. Code Methodologies for Benchmark

At Argonne, the WIMS9 lattice code was employed for the lattice (fuel element) calculations and to generate the cross sections utilized in whole-core calculations performed using the REBUS-3/DIF3D code package. The WIMS9 code calculations utilized a 172-group cross section library based on JEF2.2 data. In this approach, the CFP is explicitly represented in a fuel compact model and the homogenized compact cross sections generated in this first step are used in a fuel element transport theory calculation using the collision probability approach in a second step. The 23-group homogenized cross sections from this step are in turn employed in the core depletion model utilizing 40 total burnup zones; 10 axial layers in each ring.

Lattice calculations and associated cross-section generation have been done using the APOLLO2 Version 2.7 code at CEA; the whole-core cylindrical-Z (R-Z) calculation is also performed with APOLLO2. The lattice calculations were performed with a collision probability module that employs a 172-group cross library based on JEF2.2 (CEA93_V7, P0 corrected). Both multicell and slab models, employing explicit representation of the CFP, were developed for generating 20-group cross sections for the whole-core calculations. The slab model was primarily created for efficiency reasons, but also offered the opportunity to evaluate the impact of different approximations on the whole-core results (e.g., effect of graphite reflector on fuel-element spectrum).

## 4. Results

The multiplication factor ($k_{inf}$) and double heterogeneity effect calculated by the participants for the initial cold state are summarized in Table 3. The reference solutions are obtained from MCNP4C calculations (ENDF/B-VI data) using one-million neutron histories. In the MCNP4C heterogeneous calculation, the fuel particle distribution in the fuel compact is explicitly modeled

and the result is obtained by averaging the values from four calculations with different random particle distributions. In the homogeneous model, the fuel particles are not explicitly represented, but are spatially homogenized with the graphite matrix. The $k_{inf}$ results from ANL-WIMS9 and CEA-APOLLO2 (multicell) calculations are similar to the reference solutions; the largest discrepancy is obtained for the homogeneous case (0.6%Δk/k). The MCNP4C results indicate that the double heterogeneity effect of the DB-MHR fuel element is 13.1%, which is about a factor of five higher than that observed for enriched uranium fueled VHTRs. This larger effect is due to the use of transuranics (plutonium and minor actinides) in the DB-MHR design. The deterministic codes estimated a similar magnitude for the double heterogeneity effect.

**Table 3:** Multiplication Factors for Fuel Element at Initial Cold State (Phase 1).

| Code | Double heterogeneous model | Homogeneous model | Double heterogeneity effect (%Δk/k) |
|---|---|---|---|
| MCNP4C | 1.21027 ± 0.00075 | 1.05159 ± 0.00065 | 13.1 |
| ANL-WIMS9 | 1.21040 | 1.05752 | 12.6 |
| CEA-APOLLO | 1.21434 | 1.05832 | 12.8 |

*ANL-WIMS9 solutions obtained with 172-group compact and element calculations.

The normalized power distribution (fission rates provided by CEA) in the fuel element at the cold state (Phase 1) has been calculated by the codes and compared. The power distributions from the WIMS9 and APOLLO2 calculations were found to be similar to those from the MCNP4C calculations (within $2\sigma_{MCNP}$, $\sigma_{MCNP}=\pm 0.01$). It was also found that the distribution is slightly peaked at the fuel element periphery due to the higher moderation in this region (peak = 1.07). The agreement in the calculated power distributions of the hot irradiated states is similar to that of the cold state. However, for the very high burnup states (e.g., 600 GWd/t), a flatter power distribution (peak = 1.01 versus 1.07) is observed.

The spectra for the Phase 1 (initial cold state) and 2 (hot and depletion) fuel elements are compared in Fig. 3. For the initial cold state, the spectra calculated by the deterministic codes are quite similar to that from the MCNP4C calculation. The thermal flux is observed to peak around 0.1 eV. Flux depressions are seen around 0.3 and 1.0 eV due to the resonances of Pu-239 and Pu-240. Typically, the hot-initial-state thermal flux of the enriched uranium fueled VHTR peaks around 0.3 eV due to the high operating temperature. However, because of the resonances of the transuranics in the DB-MHR fuel, a thermal flux spectrum different from that of the uranium fueled VHTR is obtained; i.e., no significant peak is observed near 0.3 eV and the thermal flux level is low. It is interesting to note that since about 60% of the heavy metal nuclides and most of the Pu-239 (97%) and Pu-240 (67%) have been consumed after a burnup of 600 GWd/t in the DB-MHR, the flux spectrum is totally different from that of the initial state. The thermal flux depression is no longer observed, indicating the reduction in the resonance effect of the heavy metal nuclides. The CEA result shows a slightly higher thermal flux peak, for this high burnup state. Consequently, the multiplication factor calculated by the CEA is slightly higher at this burnup point (see Table 3 and Fig. 3).

The multiplication factors calculated by CEA and ANL for Phase 2 are summarized in Table 4. At the initial state, the difference between the ANL-WIMS9 and CEA-APOLLO2 results is about 0.15%Δk/k, while it is about 0.34%Δk/k at 600 GWd/t. The hot state predictions of the two codes are therefore quite similar.

**Figure 3:** Fuel Element Flux Spectra of Phase 1 and 2.

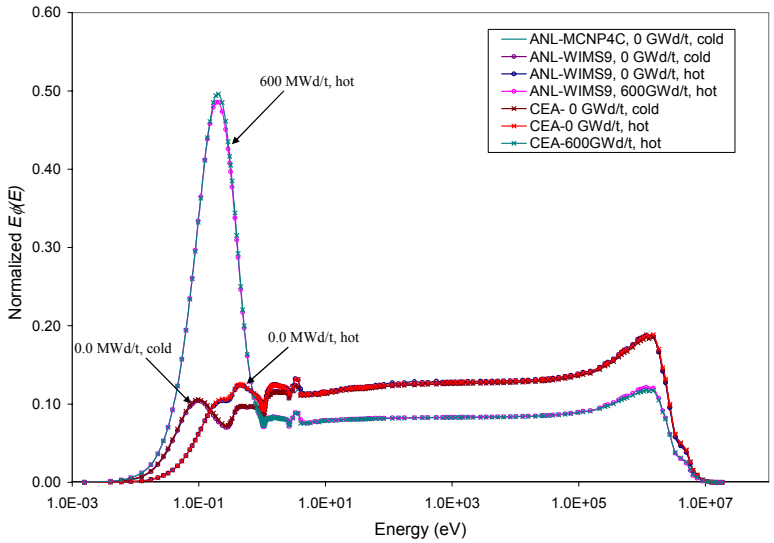


**Table 4:** Multiplication Factors for Hot Fuel Element Depletion Cases (Phase 2).

| Conditions | ANL-WIMS9 | | CEA-APOLLO2 | |
|---|---|---|---|---|
| | 0 GWd/t | 600 GWd/t | 0 GWd/t | 600 GWd/t |
| Hot | 1.12534 | 0.93059 | 1.12708 | 0.93380 |
| Cold | 1.21051 | 0.83160 | 1.21434 | 0.83543 |
| Defect (pcm) | 6252 | -12792 | 6376 | -12610 |

*ANL-WIMS9 solutions obtained with 172-group compact and 23-group lattice calculations.

In Table 4, the temperature reactivity defect was estimated as the difference in the multiplication factors of the cold and hot conditions. The temperature reactivity defect is positive at the initial state, while it is negative at 600 GWd/t. The value at the high burnup state implies that an increase in temperature results in an increase in the reactivity, which is undesirable from a reactivity control viewpoint. There are two primary reasons for the trend of the temperature defect: Doppler component (positive contribution as temperature is decreased) and the spectral component (negative). The Doppler component, arising from the transuranics, primarily Pu-240, is predominant at the initial state. At the high burnup state (600 GWd/t), at which point the leading Doppler (transuranic) contributors have been depleted, the spectral component dominates. In the actual DB-MHR designs proposed by General Atomics, a certain amount of burnable absorber, such as erbium is retained in the fuel element at the high burnup state to ensure a reduction in reactivity with temperature increase.

The burnup-dependent multiplication factor and nuclide number densities are compared in Fig. 4 and Table 5, respectively. The overall trend of the multiplication factor curves from the ANL-WIMS9 and CEA-APOLLO2 calculations are similar, but the multiplication factor from the CEA calculation is slightly higher at high burnup. The estimated number densities of plutonium isotopes from the two code systems are also quite similar. However, a significant

difference is observed in the estimated number density for Am-242m (and to a lesser degree Pu-242), which tends to make the differences between the number densities of some of the higher actinides larger and increase with burnup. The discrepancy in the Am-242m number density was found to be due to the different branching ratios used to represent the Am-241 neutron capture event in WIMS9 and APOLLO2 calculations (0.10 and 0.115, respectively).

**Figure 4:** Multiplication Factor ($k_{inf}$) Curve for Fuel Element (Phase 2).

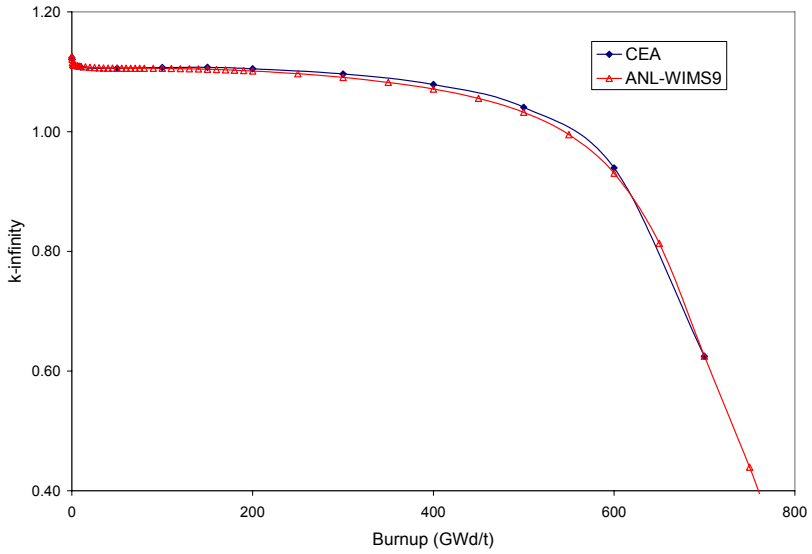


**Table 5:** Relative Differences in Estimated Number Densities (%) for Phase 2.

| Isotope | 100 GWd/t | 200 GWd/t | 300 GWd/t | 400 GWd/t | 500 GWd/t | 600 GWd/t |
|---|---|---|---|---|---|---|
| Pu238 | -0.5 | -0.7 | -0.8 | -0.9 | -0.9 | -1.0 |
| Pu239 | -0.1 | 0.2 | 0.1 | 0.1 | -0.8 | -2.4 |
| Pu240 | -0.1 | -0.1 | -0.1 | -0.1 | -0.2 | -0.9 |
| Pu241 | 0.1 | -0.1 | 0.0 | 0.0 | -0.3 | -0.7 |
| Pu242 | -0.5 | -1.0 | -1.4 | -1.6 | -1.7 | -1.7 |
| Am241 | -0.2 | -0.2 | -0.4 | -0.4 | -0.9 | -1.8 |
| Am242m | 14.0 | 15.0 | 15.7 | 16.0 | 15.2 | 14.1 |
| Am243 | 1.8 | 2.9 | 3.5 | 3.7 | 3.8 | 3.9 |
| Cm242 | -1.3 | -1.8 | -1.8 | -2.0 | -1.8 | -2.1 |
| Cm243 | -1.0 | -1.5 | -1.6 | -1.7 | -1.7 | -1.8 |
| Cm244 | 0.3 | 1.3 | 2.4 | 3.2 | 3.8 | 4.0 |
| Cm245 | 0.4 | 1.0 | 2.0 | 2.9 | 3.5 | 3.7 |

The estimated TRU consumption rates of the DB-MHR core are compared in Fig. 5. For this comparison, the ANL mass balances were obtained from an equilibrium core analysis using the REBUS-3/DIF3D code. On the other hand, CEA obtained the mass balances after seven recycles of the TRU fuel in the DB-MHR core, from a non-equilibrium calculation. Additionally, the ANL calculation used a cylindrical-Z core model, while CEA used slab (heterogeneous description) and cylindrical-Z (homogeneous description) core models. The cycle length of the equilibrium core is estimated as 286.3 days by the ANL REBUS-3 calculation. Generally, the results are quite consistent. The total heavy metal consumption rates calculated by ANL and CEA are 58.8% and 58.4%, respectively.

**Figure 5:** TRU Consumptions in DB-MHR (%).

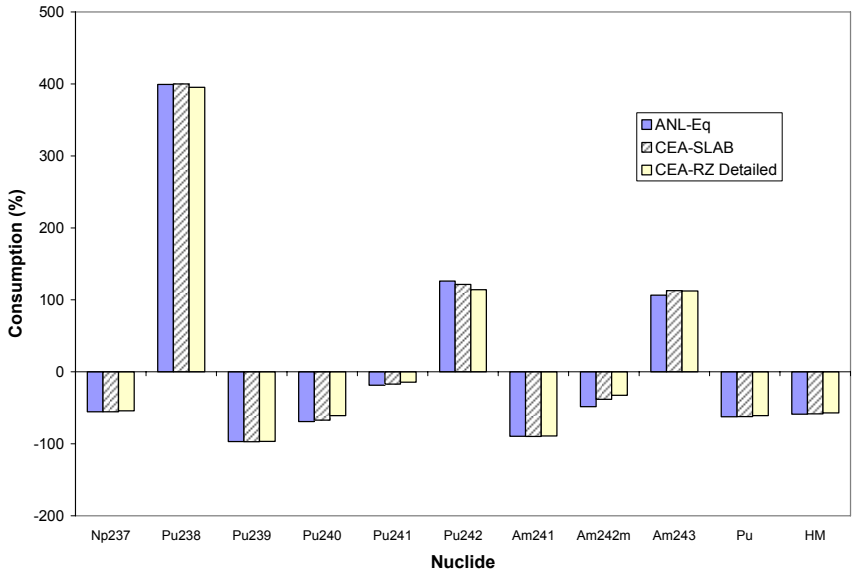


Finally, it is noted that ANL predicted $k_{eff}$ values of 1.054 and 1.0006 for the beginning and end of the equilibrium cycle, respectively. The CEA results for the core $k_{eff}$ were quite similar (differences of 0.2% and 0.33% at beginning and end of the equilibrium cycle, respectively).

## 5. Conclusions

A benchmark problem for the DB-MHR core design was developed for the purposes of (1) confirming the high TRU consumption and (2) evaluating the impact of differences in code methodologies and nuclear data files on core physics results. Currently, only results from ANL using WIMS9/DIF3D/REBUS-3 and MCNP4C and CEA using APOLLO2 have been intercompared. Generally, good agreements were found between the results of the codes.

## Acknowledgements

This work was supported by the U.S. Department of Energy under Contract number W-31-109-Eng-38. The French CEA support for this work is also greatly appreciated.

## References

1) T. K. Kim, T. A. Taiwo, W. S. Yang, R. N. Hill, and F. Venneri, "Assessment of Deep Burnup Concept Based on Graphite Moderated Gas-Cooled Thermal, Reactor," Proc. PHYSOR 2006 – Advances in Nuclear Analysis and Simulation, Vancouver, British Columbia, Canada, September 10-14, on CD-ROM, American Nuclear Society, Lagrange Park, IL. (2006).
2) Potter, and A. Shenoy, "Gas Turbine-Modular Helium Reactor (GTMHR) Conceptual Design Description Report," GA Report 910720, Revision 1, General Atomics, July 1996.